MONITORING OF ENVIRONMENTAL CONDITIONS IN TAIGA FORESTS USING ERS-1 SAR DATA: RESULTS FROM THE COMMISSIONING PHASE

Eric Rignot, Jo Bea Way, Kyle Mc Donald,

Jet Propulsion Laboratory
California Institute of Technology
Pasadena CA 91109 USA

Leslie Viereck, Cynthia Williams, Phyllis Adams, Cheryl Payne, William Wood,

Institute of Northern Forestry
U.S. Forest Service
Fairbanks, AK 99701 USA

Jiancheng Shi

Department of Geography
University of California, Santa Barbara
Santa Barbara, CA 93106 USA

Corresponding Author:

Dr. Eric Rignot

Jet Propulsion Laboratory

California Institute of Technology

MS 300-243

4800 Oak Grove Drive

Pasadena, CA 91109, USA

Ph (818) 354-1640

FAX (818) 393-6943

E-mail: eric@adelie.jpl.nasa.gov

Abstract

The European Space Agency first Remote Sensing Satellite, ERS-1, offers the first opportunity to monitor a complete seasonal cycle for an Alaskan forest ecosystem using a spaceborne C-band frequency ($\lambda = 5.7cm$) VV-polarization (vertical transmit, vertical receive) synthetic aperture radar. During the 3-day repeat Commissioning Phase of ERS-1, from August 1991 to December 1991, ERS- 1 SAR data were collected in the region of Manley Hot Springs, Alaska, along the Tanana River, west of Fairbanks. In parallel with the SAR data collection, meteorological data from three weather stations positioned in three forest stands, along with *in situ* measurements of the dielectric and moisture properties of the canopy and of the ground cover have been collected. The *in situ* data collection was in floodplain forest stands dominated by balsam poplar, white spruce, and black spruce.

The largest changes in radar backscatter (about 3 to 4 dB) are detected in early winter as a result of freezing of the soil and vegetation, These changes are explained using radar backscatter models and are due to large changes in the dielectric properties of the soil and vegetation as the trees and the soil freeze. Smaller changes in the dielectric properties of the soil and vegetation occur in the summer when periods of heavy rain showers give way to periods of warm, sunny, and dry conditions, and ERS-1 radar backscatter values typically drop by 1 to 2 dB during those summer transitions. In winter, dry snow covers the ground and the radar backscatter values increase again by 1 to 2 dB. Phonologic changes are more difficult to detect but deciduous trees show a different temporal radar response after leaf fall. Finally, examination of the separability in radar backscatter of different tree species indicates that ERS- 1 has only limited capabilities for mapping forest types.

1 Introduction

Synthetic aperture radars have shown considerable potential for monitoring soil and vegetation moisture of the Earth's surface (e.g. Ulaby et al., 1982, and 1986) because of their penetration capability through dense vegetation canopies and top layers of the soil surface, and also because of the strong dependence of the radar backscatter on the dielectric properties of the surface, which are controlled by the moisture status of the soil and vegetation. With the launch of ERS-1 SAR, we have, for the first time the opportunity to monitor both changes in the water status of the soil and vegetation as a result of changing environmental conditions, and changes in the vegetation phenology as a result of seasonal growth and senescence, over long periods of time, and at short revisit intervals. In the Arctic, where the effects of climate change on terrestrial ecosystems are expected to be the greatest (Manabe and Wetherald, 1980; Hall, 1988), the ability to monitor these changing seasonal conditions of a forest canopy from space may be an essential tool for assessing the effect and/or response of boreal forests to longer-term climate shifts.

Past studies have shown that several time-variant events may result in significant changes in radar backscatter from terrestrial ecosystems. These events include: 1) changes in the geometric characteristics of the vegetation cover, for example from clear-cutting of forests, crop harvesting, leaf senescence or fall in deciduous trees; 2) changes in the surface roughness of the reflecting surface, for example as a result of soil erosion, or as a result of wind roughening or ice formation on areas of standing water; 3) changes in the soil and vegetation moisture due to precipitation, changes in the moisture status of the ground layer (Way et al., 1992a), or freeze/thaw transitions (Way et al., 1990).

Most of the research accomplished to date on temporal changes in forest radar backscatter has been based on airborne SAR observations, Dobson et al. (1991) compared the radar intensity signatures obtained by the NASA/JPL three-frequency polarimetric airborne SAR, AIRSAR, (van Zyl et al., 1992) collected over mixed conifer and hardwood forest of northern Michigan in early spring (1 April 1990) and mid-summer (10 July 1990), and concluded that phonologic changes of the vegetation over that period resulted in the following changes in the radar signature: (1) for pine stands, a slight decrease (1 to 2 dB) in image intensity at P- and L-bands ($\lambda = 68cm$ and $\lambda = 24cm$, respectively) and a slight increase (1 dB) at C-band ($\lambda = 5.6cm$); and (2) for deciduous stands, a decrease in radar backscatter at all frequencies, with the greatest decrease at P-band (2 to 4 dB) and the least at C-band (O to 2 dB). These differences were attributed to changes in the dielectric properties of the tree branches and trunks, and an increase in the foliar biomass.

Dobson et al. (1991) also studied the impact of rainfall on SAR signatures from forested stands, and found that the radar backscatter increased by O dB at P-band, 1 to 2 dB at L-band, and 2 to 3 dB at C-band due to rain, largely due to the increase in intercepted moisture present in the tree crown.

A series of multitemporal AIRSAR data sets were acquired over the Bonanza Creek Experimental Forest (BCEF) near Fairbanks, Alaska, in March of 1988 and May of 1990 (Way et al., 1990, 1992a, and 1993; Dobson et al., 1993; Kwok et al., 1993). P-, L- and C-band data were acquired on five different days over a period of two weeks in March 1988 and on three different days in May 1991. During the time period over which the SAR data were collected, the environmental conditions changed significantly. In March 1988, temperatures ranged from unseasonably warm (1 “C to 9°C)

to well below freezing (-8°C to - 15" C), and the water in the snow and trees changed from a liquid to a frozen state. Bole dielectric properties and snow wetness changed significantly with these changing temperatures. The SAR data clearly indicate the radar return is sensitive to these changing environmental factors. Analysis of the L-band SAR data shows a 1 to 6 dB increase (depending on polarization and canopy type) in radar backscatter of the forest stands under the warm conditions relative to the cold,

With respect to the AIRSAR imagery collected in May 1991, there was still snow on the ground and the soil was still frozen. On May 4th, the river was breaking up and ice jams caused flooding on the lower terraces dominated by alder and balsam poplar stands. By May 7th, the ice jams had broken and the forests drained. The change in radar backscatter between the flooded and drained forests was 5 dB at L-band and the dominant scattering mechanism as determined by van Zyl (1989) and from radar backscatter models changed from dominant trunk-ground interactions for the flooded forests to diffuse scattering from the canopy foliage for the drained forests.

The European Space Agency first Remote Sensing Satellite, ERS-1, launched in July 1991, operates a synthetic aperture radar instrument at C-band frequency ($\lambda = 5.7cm$), VV-polarization (vertical transmit and receive polarization), 23° look angle, and 30m resolution (Attema, 1991). The steep look angle of ERS-1 contrasts with the look angle of AIRSAR which usually lays about 50°. Scattering mechanisms and magnitudes of changes in radar backscatter are expected to vary significantly between these two look angles. ERS-1 is also the first SAR instrument to offer the opportunity to observe changes in radar backscatter from an Alaskan forest ecosystem throughout an entire seasonal cycle.

The questions addressed in this paper are (1) What arethe magnitudes of seasonal variation in the C-band VV polarization 23° microwave backscattering coefficient in response to naturally occurring temporal variability in taiga forest stands ?, (2) How are these variations in the backscatter coefficient quantitatively related to specific forest stand and environmental properties via the relevant scattering mechanisms ? (3) Given the observed temporal variations in backscatter and the associated calibration limitations, what ecologically useful information can be inferred from multitemporal SAR observations ?

The paper is organized as follows. Section 2 describes the ERS- 1 mission. Section 3 presents our test site near Manley Hot Springs during the Commissioning Phase. Section 4 describes the SAR data, the data calibration, the registration of multitemporal data, and the extraction of multitemporal radar backscatter values from selected forest stands. Section 5 describes the ground truth data collection which includes static tree characteristics, weather data, and temporally varying soil and vegetation properties. Section 6 discusses radar backscatter model predictions for ERS-1 SAR using the Michigan microwave canopy scattering model (MIMICS) (Dobson et al,, 1989; Ulaby et al., 1990). Section 7 presents the radar backscatter observations and discusses the relation between temporal changes in radar backscatter and changes in the environmental and phonologic conditions. Section 8 presents our conclusions.

2 The ERS-1 mission

ERS-1 SAR data may only be acquired in view of a ground receiving station as no recording capability exists on-board the spacecraft, In this paper, we address data collected and processed by the Alaska SAR Facility (ASF) at the University of

Alaska's Geophysical Institute in Fairbanks, Alaska (Carsey and Weeks, 1987). ERS-1 currently follows a sun-synchronous polar orbit at amean altitude of 785 km with a 35-day repeat cycle until early 1994. Data from this Multidisciplinary Phase can be used to monitor temporally varying surface properties on about one week intervals depending on the latitude of the region of interest. The Commissioning Phase of the orbit during the first 5 months of the mission (August 3- December 15) was an exact 3-day repeat orbit which, for some parts of the world, provided identical coverage every three days, In Alaska, the 3-day repeat tracks transected the center of Alaska crossing the Tanana River near a town called Manley Hot Springs. There is currently no ongoing forest research in this area however the frequent repeat coverage was so unique that we made an extra effort to obtain adequate surface data such that the ERS-1 Commissioning Phase data would be useful. During the current 35-day repeat orbit which started on April 14, 1992, we have shifted our test site to the Bonanza Creek Experiment Forest, where an abundance of other forest research is ongoing (there are two Long-Term Ecological Research (LTER) sites in Bonanza Creek) and where, due to its proximity to the Institute of Northern Forestry and the University of Alaska, the logistics associated with collecting surface data during an ERS- 1 overpass are significantly easier.

3 The Tanana Valley forests

The test site representing the Alaskan taiga in this study is called "Manley Hot Springs"; however the actual stands which were monitored are about 40 km down-stream from the town of Manley Hot Springs. Figure 1 shows the location of the Manley site on a map of Alaska along with the ground track of ERS- 1 swath. The

specific stands were selected to be essentially at the center of the 3-day repeat ERS-1 swath, at a center latitude longitude location of 65 °03'N and 151° 10'W. The site is along the Tanana River in the zone of discontinuous permafrost. The climate is continental with large diurnal temperature changes, low precipitation, low cloud cover, and low humidity. The Manley site includes both upland fire-controlled succession and floodplain succession forests. The floodplain forests are the focus of this paper in order to eliminate topography as a factor in the image analysis, particularly with respect to the 23° look angle of ERS-1.

Due to active erosion of mature stands along the Tanana and production of silt bars on the river floodplains, most floodplain forest stands tend to be in a variety of young successional stages (van Cleve and Viereck, 1981; Foote, 1983). Primary succession on the floodplain begins with willow and alder which stabilize the terraces providing biological control of the flooding and allowing the forest floor to develop (van Cleve and Yarie, 1986; van Cleve et al., 1991). Alder (*Alnus tenuifolia*) are followed by balsam poplar (*Populus balsamifera*) which compete with the shade-intolerant alder. Finally, white spruce (*Picea glauca*) dominate on river alluvium where permafrost is absent. In locations where the white spruce stands are protected from erosion, their shading allows the formation of permafrost which then results in a final successional transition to black spruce (*Picea mariana*). The uplands are dominated by aspen, paper birch, and black spruce forests,

The coldest month is January with a mean daily temperature of -24°C; July has a mean daily temperature of + 17°C. On any given date, the extremes of temperature can vary by as much as 35°C (in June) to 65°C (in January). Rainfall occurs mostly in July and August, with the heaviest and most frequent precipitation in August

(Viereck et al., 1983; van Cleve et al., 1983; Vierecket al., 1986; Slaughter and Viereck, 1986; Viereck and Adams, 1990; and Juday and Dyrness, 1985). Flooding during springbreakup occurs mostly along therivers, butmay cover broad areas of the lowland floodplains. Occasional summer floods from excessive rain and glacier melt occur in August. Fire is aregular and important element of the natural environment. The fire season extends from mid- to late-May through early October with the peak from June 10 to July 20.

A unique feature of this high-latitude setting is the discontinuous permafrost which underlies much of the region. The depth of the thawed "active" upper level varies with season. Impeded drainage caused by the presence of permafrost and the short growing season helps keep the Alaskan interior from being a desert, despite the low annual precipitation. Snow in the Fairbanks area generally covers the entire landscape from October through mid-April, but does not commonly exceed 25 cm water equivalent annually: too shallow to reach up to the lower branches of medium to large trees. The snow forms a dry ground mat that ablates in winter primarily by sublimation, and which is characterized by a low density and a high percentage of depth hoar (Pruitt, 1984).

4 ERS-1 SAR data

4.1 Data reception and processing

ASF generates various types of SAR products corresponding to different pixel spacings, and spatial and radiometric resolutions. The SAR data analyzed in this paper are 'high-resolution" products, with a signal amplitude coded on 8-bits, 4-looks in

azimuth, l-look in range, 12.5m pixel spacing in both slant-range and azimuth, corresponding to 27m and 29m resolution in azimuth and slant-range respectively, and covering a 100 km x 100 km area. We acquired 22 images of the Manley site between DOY 224 and DOY 341 during descending passes of ERS-1, that is at about 1:00 pm Alaska daylight time; and 15 images during ascending passes of ERS-1, that is at about 1:00 am Alaska daylight time.

4.2 Data calibration

As part of ERS-1 Commissioning Phase, NASA organized a vast campaign to calibrate the SAR data collected by ERS- 1 and received and processed at ASF (Fatland and Freeman, 1992). Corner reflectors were deployed at three different locations, near Toolik Lake north of the Brooks Range, near the Delta Junction south-east of Fairbanks along the Tanana river, and between Tanana City and Manley Hot Springs west of Fairbanks along the Tanana river. The corner reflectors provided an opportunity to calibrate ERS- 1 SAR data early in the mission, that is, determine the antenna pattern correction necessary to maintain a good radiometric fidelity of the data across range in each scene, and determine the gain factor to apply on the data to obtain calibrated radar backscatter values. These calibration factors are now incorporated into the ASF/SAR processor, so that all ERS- 1 SAR data are processed in a consistent fashion, and the users are provided with data that are already calibrated.

The ERS-1 SAR data processed at ASF are calibrated with an absolute accuracy better than 1 dB (Fatland and Freeman, 1992). The calibration uncertainty within one scene due to antenna pattern corrections is less than 0.5 dB. In the case of the repeat-pass imagery considered in this paper, antenna pattern corrections do

not affect the analysis of temporal changes in radar backscatter since each surface element is repeatedly imaged at the same incidence angle, within fractions of a degree, The entire calibration process relies in fact on the stability of ERS-1 radar gain. Ground verification of ERS-1 SAR performance by the European Space Agency (ESA) prior to launch revealed that the radar gain was stable with an accuracy better than 0.33 dB(Attema, 1991). Preliminary in-orbit verifications of ERS-1 SAR performance have not yet been able to detect radar gain instabilities greater than that value (Attema, 1992a). In addition, no day/night gain effects have been detected over ESA's transponders and over rain forest (Attema, 1992a). ERS- 1 SAR is therefore a unique tool for monitoring studies as the relative calibration accuracy between consecutive images is better than 0.33 dB, and changes in radar backscatter can be detected at the 0.5 dB level with confidence. With a noise equivalent radar backscatter (i.e. the radar backscatter of a surface at the noise level) of about -27 dB(Attema, 1992b), ERS- 1 is also capable to observe a large variety of natural targets with a high signal to noise ratio.

4.3 Registration of ERS-1 multitemporal data

During the Commissioning Phase, ERS- 1 followed very accurate 3-day repeat orbits. Every 3-days the radar, overflew the same area, at the same time of the day (± a few minutes), and with the same imaging geometry. The incidence angle of the electro-magnetic radar signal onto each resolution element was repeated within fractions of a degree, and the geometric distortions in the scene due to topographic variations were exact] y repeated. It is therefore possible to use directly slant-range SAR imagery for registration of the multitemporal observations and detection of changes in radar backscatter. There is no need for computationally expensive geometric correction

routines, resampling, and georeferencing of the SAR data.

Sub-images 1536 x 1536 pixels 'in size corresponding to our primary test site were extracted from the original 8192 x 8192 pixels high-resolution scenes and co-registered with other sub-images, Co-registration of sub-image pairs was achieved by locating the bright return from one of the trihedral corner reflector present in the scene, and determining the pixel offset between the images by correlation of the intensity returns. ERS- 1 SAR imaging geometry was stable enough between repeat passes that pixel to pixel registration could be achieved over the entire scene, without the need for rotation or stretching of the images, using only one tie-point. A similar registration accuracy using a simple translation of the image pixels is currently impossible to achieve with airborne SAR data, which illustrates the practicity of a spaceborne SAR instrument for monitoring temporal changes of the Earth surface from repeat-pass imagery,

4.4 Extraction of radar backscatter values

The three forest stands that have been monitored during the period of study are labeled BS-50 (black spruce), BP-51 (balsam poplar), and WS-52 (white spruce). For each tree stand, a corresponding polygon is drawn on the computer to extract pixel values corresponding to that area. The pixel values are converted into intensity values based on the calibration factors recorded in the data header, and the average intensity is computed for each polygon, A few additional polygons are drawn in other forests stands, in the river, and in shrub-lands (SH-51) to compare the variability in radar backscatter within tree species and in between different types of terrain cover. Figure 2 shows the location of these stands within an ERS-1 image acquired

on 08/15/91 (DOY 224) during a descending pass. The SAR image is 1536 pixels by 1536 pixels in size, and 12.5m in pixel spacing in both range and azimuth. Near-range is on the left in the figure, with ERS- 1 flying from bottom to top looking to its right.

The radar backscatter curves for the descending passes are shown in Figure 3a for four training sites, and in Figure 3b for all the stands drawn in Figure 2. Figure 3c shows the radar backscatter curves during descending and ascending passes for four training sites. The results are discussed in Section 7.

5 Ground truth data collection

5.1 Stat ic properties

Static canopy parameters for BS-50, BP-51, and WS-52 were collected in July 1991 by the U. S.D.A. Forest Service Institute of Northern Forestry and by a group of Earthwatch students (Williams, 1992). The data set includes diameter at breast height (DBH), tree height, density (trees/ha), age, surface roughness description, understory cover and description.

In each stand, a single transect was used to locate plots. Aerial photographs were used to determine the transect starting points and transect directions for the stands. Plots were placed 100 m from each other except when anomalous vegetation (such as is found in old sloughs) would have been included within a plot; direction was determined with a hand-held compass. Ten plots were sampled in each stand, with each plot including at least 40 trees were measured. Plot radii were chosen to include roughly 15 live trees. A “tree” has a DBH of at least 2.5 cm. All tree DBH were

measured. In each stand, 40 trees of the dominant overstory species that did not show signs of growth disturbance were chosen for height measurements. Each tree for which height measurements were made was also cored with an increment borer for determination of age. Cores were temporarily stored in straws and later mounted on wooden holders and sanded. Rings were counted and the depth of the cork cambium, phloem, cambium and active xylem were determined. The depth of the organic layer was measured using a meter stick at each plot. This measurement was taken from the surface to the first mineral soil layer and included any live mosses and lichens from the forest floor.

Table 1 shows a summary by stand of density, percentage cover, mean DBH, mean height, basal area, and biomass, The black spruce stand exhibits the greatest density, but because of its small size and cover contains less woody plant basal area and biomass than the other stands.

5.2 Weather data

5.2.1 Within stand weather data

Weather data were obtained in each of the three Manley stands using an Easylogger data logger with an Eprom data storage pack, a quantum PAR sensor, a Physchem temp/RH probe, and three direct burial soil temperature probes, In addition, a rain gauge was placed in the open near the campsite which was the base for multitemporal measurements.

Figure 4a shows the air temperature recorded in BS-50 between DOY 220 and DOY 365. Symbol markers in Figure 4a indicate the dates of availability of ERS-1 SAR

measurements. August (DOY 213 to 243) is relatively warm. The first night-time " sub-zero air-temperatures are detected in September (DOY 244 to 273), and the first day-time sub-zero air-temperatures occur around mid-october (DOY 290). Air-temperatures are very low in November (DOY 305 to 334), with small occasional warmings, and are in the -2 O'sOC in December. Data were only collected between DOY 219 and DOY 257 in WS-52 and between DOY 219 and DOY 284 in BP-51 because of instrument failure. During the period of coincident measurements, the air temperatures in all tree species were very similar. The correlation coefficient is 0.95 between BS-50 and WS-52 with a standard deviation of the difference of 1.9°, Between BS-50 and BP-51, the correlation coefficient is 0.96 and the standard deviation of the difference of 1.8°.

Figure 4b shows the solar radiation measurements in BS-50 at the times of ERS-1 descending pass. August and September are sunny and warm, with a few cloudy days (low solar radiation level). From earl y October to December the solar radiation level decreases steadily to very low values, but after the first snow fall (DOY 290) the measurements are not reliable because the sensors got covered with snow, Figure 4c shows the soil temperature at 10cm and 20 cm depth in BS-50 at the times of ERS-1 descending and ascending passes. The soil temperature at 10 cm depth is slowly decreasing from August to December in BS-50. Soil temperatures in WS-52 and BP-51 (not shown in this paper) are relatively higher than those recorded in BS-50 because black spruce trees lay on cold permafrost. Soil temperatures in BP-51 are slightly higher that those in WS-52 because the white spruce canopy is more closed and allows less incoming solar radiation to heat the ground. Figure 4d shows the precipitation rates recorded near the campsite on a few dates between DOY 219 and 252.

A subjective description of weather conditions at time of overflight and of data collection was made on those same dates, including clouds, rain, wind, dew, leaf color and phenology.

5.2.2 Airport weather data

Airport weather data were collected from the Tanana airport at the western edge of the swath, and the Manley airport at the eastern edge of the swath, The data collected in Tanana include visual observations, minimum-maximum air temperatures, precipitation rates, and snow depth. The weather reports from Manley airport include visual observations only. The air temperature measurements from Tanana airport are similar to those recorded in BS-50. Figure 5a shows the precipitation rates in Tanana noted at 3:OOpm each day, in close agreement with those recorded in Manley on the dates of data collection although the values recorded in Manley are slightly lower. On DOY 215, the precipitation rate recorded at Tanana was 149mm (not shown in the plot), the highest of the summer season. Figure 5b shows the snow depth recorded in Tanana at 3:OOpm on each day. The dates of first snow appearance and major snow storms are assumed to be valid for the Manley forest site since they were also recorded at Manley airport. The snow depth in Tanana is used as a proxy indicator of the snow depth in Manley.

5.3 Temporally varying canopy and soil properties

Temporally varying properties were collected during day-time passes of ERS- 1 for WS-52, BS-50, and BP-51, including dielectric constant profiles of the tree trunks, moisture content of the leafy vegetation, understory, and forest floor, tree water

potential, and bole temperature.

Three dielectric constant profiles at 4 depths were obtained in each stand: bark (O. 0cm), phloem (0.3cm), cambium(0.6cm), xylem (1.6cm, i.e. about 1cm into active xylem). Each measurement set was preceded by calibration with alcohol and water. The real part of the dielectric constant at 4 depths is shown in Figure 6. Bark has a low dielectric constant, so the radar signal penetrates through it with little attenuation and is mostly sensitive to phloem and cambium which are both characterized by a high dielectric constant, with little fluctuations between August and September in all tree species. The dielectric constant of phloem is highest on DOY 220 after a period of heavy rain fall (see Figure 5a) and also between DOY 235 and 239 during which the weather conditions were clear and sunny after a period of heavy rain falls on DOY 230 (see Figure 5a).

Three water potential samples per stand were recorded. Water potentials in August/September were typically high during the day ERS-1 overflight (typically -11 bars) and low during night passes (typically -5 bars).

Three samples of the leaves/needles, branches, bark, xylem; and understory (shrubs and herbaceous plants), litter, moss, organic soil, and mineral soil were collected and weighed in the field. A 1,2 cm diameter corer was used to collect the bole samples. The samples were then transported to the Institute of Northern Forestry via mail plane, dried and weighed. Figure 7a-c show the gravimetric moisture content (i.e. the ratio (wet weight - dry weight) / dry weight) of the canopy (i.e. leaves, wood, outer-bole, and inner-bole) for BS-50, BP-51, and WS-52 between DOY 220 and 252. Each point was obtained from the average of measurements taken at one to four locations (measurements were not systematically available for each plot in each stand).

The results show that the moisture values of the trees and canopy did not change significantly during that period. Figure 7d-f show the gravimetric moisture content of the surface cover (i.e. understory, litter, moss, organic soil, and mineral soil) for the same three stands. The moisture content of the litter and moss in coniferous forests changed dramatically during the period of observation. In BP-52 fluctuations in moisture content of the soil are also seen in the organic and mineral soils, due to the absence of the highly water absorptive moss layer in BP. These moisture content measurements indicate that a wet to dry transition occurred between DOY 220 and DOY 250 which is consistent with the meteorological observations which report clear and sunny skies and no rain during that same period. A return to wet conditions is observed after DOY 250 due additional rain falls. Changes in moisture content are again mostly happening in the surface cover and not in the trees or leaves,

Droplets of water present on the leaves or needles after a rain shower are not accounted for in the moisture measurements shown on Figure 7. These suspended droplets and fine film of water deposited on the canopy and understory will however strongly influence the radar backscatter from the trees according to radar backscatter models, and will act on radar backscatter as if the moisture content of the leaves was actually higher. The effect may also be time critical depending on the time lapse between the rain shower and the SAR overflight. In an experiment on wheat canopies, Allen et al. (1984) showed that the spraying of the canopy by water resulted in an immediate large increase in radar backscatter from the canopy which then decreased to its original level after a few hours as the surface water of the leaves evaporated. The same effect is expected from tree canopies, especially in deciduous trees since the leaves intercept more water from rain showers than the thin and elongated needles of conifers. Hence, it is important to complete the vegetation moisture measurements with a description

of the state of wetness of the outer surface of the leafy vegetation.

Bole temperature was recorded in each stand on one tree, always on the east side of the tree, from DOY 218 to DOY 251. The depth of the thaw of the active permafrost frost layer was recorded in 10 locations in each stand from DOY 224 to DOY 251. A photograph using ASA 200 color print film and a 50 mm lens was obtained at each stand. Each photograph was taken facing north and from the same spot.

6 Modeling results

The Michigan microwave canopy scattering model (MIMICS) (Dobson et al., 1989; Ulaby et al., 1990) is used to model the radar backscatter from various types of trees at C-band frequency, VV-polarization, and 23° look angle, MIMICS models a forest canopy as two distinct horizontal vegetation layers comprised of leaves and branches, and tree trunks, over a dielectric ground surface. The model requires both static properties of the trees and ground such as structure and geometrical characteristics, and dynamic properties such as moisture content of the soil and vegetation, and snow extent and characteristics in the winter. It was not possible to monitor all these variables during the period of study at Manley Hot Springs due to the harsh conditions in the winter, the remote location of the site from our prime site of study, and the difficulty of the logistics at that site. A finer monitoring of the soil and vegetation characteristics is currently underway at the Bonanza Creek Experimental Forest during the 35-day Multidisciplinary Phase of ERS-1.

In this section, we discuss the sensitivity of ERS- 1 radar backscatter from taiga forests as predicted by MIMICS for a range of soil and vegetation moisture conditions, The

objectives are to determine the magnitude of the different scattering components contributing to total radar backscatter from taiga forests, and to estimate the sensitivity of the total radar backscatter to the water status of the soil and vegetation. The results help interpret the ERS-1 observations, and help predict changes in radar backscatter that could be observed during the rest of the year.

We do not have yet a complete geometrical and electrical characterization of the forest floor in the different tree stands and a radar backscatter model that can accurately account for the coupling and interactions between the different layers. Instead, the forest floor is modeled as an electromagnetically equivalent bare surface whose roughness characteristics are selected in order to match the ERS- 1 radar backscatter measurements in shrub-lands given the soil moisture conditions. The same roughness conditions (rms height and correlation length) are used to model the forest floor in the other stands, as a first order approximation.

In the simulation, the volumetric soil moisture varies between 0% (very dry or frozen soil) and 40% (very wet soil at the limit of saturation). The dielectric constant of the woody material (tree trunks, branches, and needles are all assumed to have the same dielectric constant) varies between 4 (tree frozen at depth as measured in March 1988 (Way et al., 1990)) and 46 (wet flooded tree as measured in May 1991 (Way et al., 1992a)). The dielectric constant of the soil is computed from its volumetric moisture content using the equations derived by Hallikainen et al. (1985) and a soil texture of 10% sand and 30% clay. The real and imaginary part of the dielectric constant of the vegetation material (i.e. leaves or needles, trunks, and branches) are computed from the volumetric moisture content of the vegetation using the model of Ulaby and El-Rayes (1987),

The results are shown in Figure 8. The dynamic range of radar backscatter values due to fluctuations in soil moisture is about 4 dB, and the dynamic range of radar backscatter due to fluctuations in tree dielectric constant is also about 4 dB, Although C-band is mostly sensitive to the upper canopy of the forest at large incidence angles (e.g. Ulaby et al., 1986), MIMICS predicts that for taiga forests imaged at 23° look angle the soil also plays a very significant role. The effect of the soil is more pronounced in sparse canopies (BS-50) than in dense canopies (WS-52) because the signal is more attenuated by denser canopies and yields weaker returns from the ground. The effects of soil moisture and vegetation water content on the total radar backscatter are concomitant, and wetter soil and vegetation yield higher radar backscatter values than dry soil and vegetation. Given a single date observation, it is however difficult to separate the effect of the soil from that of the vegetation.

The magnitudes of the three scattering components that contribute the most to the total return from BS-50, BP-51, and WS-52, are respectively shown in Figure 8d, 8e, and 8f. These scattering mechanisms are: 1) direct scattering from the crown, 2) direct scattering from the ground, and 3) ground-trunk interactions. Other types of scattering mechanisms modeled by MIMICS such as ground-crown-ground, crown-ground, and ground-crown scattering are of second order magnitude, independent of the water status of the soil and veget at ion. Only the extreme cases of wet and dry conditions are shown in the figure to limit its complexity. The results show that for WS-52 with dry/frozen soil and dry/frozen vegetation, the radar return is dominated by direct scattering from the tree crown. If the trees and the soil become wet, the ground-trunk interactions increasingly dominate the radar return because the wet trunk-ground acts as an efficient reflector of the radar signals. The underlying forest floor has a more important contribution to the total radar backscatter in BS-50

because the canopy is more open. When the trees are frozen, the ground conditions dominate the radar backscatter. Direct scattering from the ground is significant even for wet soil and wet vegetation. In contrast, direct scattering from the tree crown is of second order magnitude. In BP-51, the sensitivity is intermediate between that of white spruce and that of black spruce. Direct scattering from the ground is important when the trees are dry/frozen, otherwise the radar backscatter is dominated by direct scattering from the crown and scattering from trunk-ground and ground-trunk interactions.

7 ERS-1 multitemporal radar observations

Between DOY 220 and 230, the trees and the soil are very wet, and, as predicted by MIMICS, the radar backscatter values are the highest (Figure 3a). The heaviest rain fall occurs on DOY 215. Subsequent rain showers DOY 220 and DOY 230 have lower precipitation rates, and the corresponding radar backscatter values are slightly lower. From DOY 230 to 250, the canopy and understory covers undergo drying as described in Section 5 from the soil and vegetation moisture measurements. The radar backscatter values of BS, SH, and WS decrease by 1.5 dB between those two dates, whereas in BP-51 the decrease is of 2 dB. On DOY 225, the BP leaves are reportedly covered with dew following a rain shower the day before, Scattering from water droplets suspended on the BP leaves may explain the increase in radar backscatter of 0.5 dB detected in BP-51 compared to three days earlier. This increase is observed in the other BP stands as well (Figure 3b), but not in conifers.

Rain occurs again after DOY 250, yielding a 1 to 2 dB increase in radar backscatter from all forest stands, especially in BP-51 where leaves are still present, although

they are now changing color before their subsequent fall. Until DOY 260, the radar backscatter values increase with increasing soil and vegetation moisture conditions as predicted from MIMICS. On the night of DOY 262, freezing air-temperatures are recorded, yielding a O.5 dB decrease in radar backseat ter the day after compared to three days earlier in SH-51 and BS-50. A larger change in radar backscatter, greater than 2 dB, is detected in SH-51 and BS-50 in the data acquired at night (Figure 3c), but little change is seen in WS-52 and BP-51. These observations indicate that freezing of the soil and of the lower vegetation probably occurs on the night between DOY 262 and DOY 263 but is yet not vigorous enough to freeze the taller vegetation. Both the soil and the vegetation thaw after DOY 263 since the radar backscatter values of all forest stands return to their initial level three days later.

With the first snow fall and the first sub-zero air-temperatures recorded during the day starting on DOY 280, the radar backscatter values abruptly decrease to reach a minimum on DOY 290. Based on the MIMICS model predictions and on earlier observations of forest freeze-thaw with airborne SAR instruments (Way et al., 1990), we attribute this drop in radar backscatter to a large decrease in the dielectric constant of the soil and vegetation due to freezing. The total decrease in radar backscatter detected during freezing is about 4 dB for SH-51 and BS-50, 3 dB for WS-52 and BP-51, hence slightly more pronounced in shrub-lands, and sparse and open canopies. After freeze-up, BS-50 and SH-51 are not separable as predicted from MIMICS since the ground conditions dominate the radar returns from BS-50 and the soil conditions in BS-50 and SH-51 are similar. The radar backscatter curves from each tree species become parallel after freezing.

Interestingly, BP trees continue freezing after DOY 290 since their radar backscatter

values continue decreasing until DOY 296, as opposed to other trees. This effect is observed in BP-51 as well in other stands of BP (Figure 3b). We observed a similar phenomena in the AIRSAR campaign of March 1988 where some BP trees froze at a slower rate than BS and WS trees, and some of them were even thawed on the frozen day (Way et al., 1990 and 1993 b). Recent bole temperature measurements of BP trees in the Bonanza Creek Experimental forest also suggest that BP trees are slowlier to respond to environmental changes and undergo fewer thaw/freeze transitions than coniferous trees (Zimmerman, 1993), It is suggested that these phenologic differences observed during freeze-thaw transitions are due to a higher sugar content in deciduous trees that lowers their freezing points (Waring, ? 992),

Changes in radar backscatter due to leaf fall are difficult to separate from those due to environmental conditions because they occur over longer time periods. However, after leaf fall (that is after DOY 270 according to visual observations), the temporal radar response of BP trees becomes similar to that of conifers, whereas important differences exist during the summer and fall months as noted earlier. These observations are consistent with the MIMICS model predictions that scattering from the crown dominates when leaves are on the deciduous trees in the summer, whereas direct scattering from the ground dominates in the absence “of leaves and when the soil and vegetation are in the process of freezing.

After DOY 290, the soil is frozen, the snow layer builds up, and the radar backscatter curves increase again, Continuous vigorous freezing of the vegetation is expected to level off the radar backscatter values from the forest in winter because once all the fresh liquid water content inside the trees is in frozen state the dielectric properties of the trees do not change any more and remain at low values. The observed increase is

radar backscatter is therefore unexpected. Due to the low air-temperatures, the snow layer is typically dry, of relatively low density, and with snow grains small in size (Pruitt, 1984). Rayleigh scattering from freshly fallen snow grains does not support the observed increase in radar backscatter at 23° look angle, and, in fact, predicts a very small negative correlation between snow depth and radar backscatter for rough surfaces since increasing snow depths results in enhanced attenuation of the radar returns from the underlying ground. Dry snow is therefore transparent to the radar signals and can at the most attenuate the radar returns. Another possibility is to have enhanced scattering from the underlying frozen ground in the same manner as bedrock covered with a thin-layer of low-loss material appears brighter to the radar due to signal refraction and changes in the effective wavelength of the signal (Elachi et al., 1984). After DOY 290, the air-temperatures drop steadily to lower values, the soil freezes to larger depths (see Figure 4c) and dries out due to fluxes of water vapor from the soil into the snow (Trabant and Benson, 1972; Sturm and Johnson, 1992). As freezing of the active layer becomes deeper, the radar backscatter from the ground is increasingly attenuated and cannot generate an increase in total radar backscatter. The process responsible for the increase in radar backscatter is therefore neither due to the fresh snow nor to the freezing ground.

A characteristic of Alaskan snow is the rapid build up of a depth hoar at the base of the snow due to the thin snow layer and the large temperature gradients between the snow/soil interface and the free-air above the surface. Ice crystals in the snow layer develop rapidly in early winter and may reach grain sizes of several millimeters whereas freshly fallen dry snow grains are typically smaller than 0.5 mm. Large ice crystals can generate sufficient volume scattering at C-band frequency, even at 23° look angle, to be detected by ERS-1 SAR. As an illustration, we ran a simulation

using a two layer snow model on top of a ground surface, where the top layer has a fixed snow grain size of 0.5mm, and the bottom layer is depth hoar, of increasing height and of varying ice crystals size, A radiative transfer model couples the two layers along with scattering from the ground to yield the total radar backscatter. The roughness characteristics of the ground are selected to obtain radar backscatter values close to those measured by ERS-1 in shrub-lands areas, i.e. about -14 dB. The results are shown in Figure 9 as a function of ice crystal size in the depth hoar and height of the depth hoar keeping the total snow depth constant equal to 20 cm, The radar backscatter values increase by several dBs with increasing grain sizes and increasing height of the depth hoar. In particular, ice crystals about 2.5 to 3.5 mm in size appear capable of generating the observed increase in radar backscatter if the height of the depth hoar slowly increases with time. Confirmation of this interpretation should be done using a surface-based radar that would indicate whether the dominant radar returns are indeed coming from the depth hoar or not.

After DOY 320, the radar backscatter curves decrease again. The air-temperatures raise a little during that period, but remain largely below zero. The soil temperature recordings indicate a slight warming of the soil at 10 cm depth during that period. This warming trend may affect the development of the depth hoar, or yield partial thawing of the top soil layers and of the understory vegetation that are protected from the cold air-temperatures by the insulating snow layer. We do not know the answer and why a slight decrease in radar backscatter is detected during that period. The radar backscatter values increase again after DOY 340 with the return of very cold air-temperatures and additional fresh snow, Changes in radar backscatter with snow depth are more pronounced in BS-50 and SH-51 where the effect of the ground is dominant than in BP and WS where radar signals from the ground are attenuated

by the canopy. Considering thesnow depth recordings shown in Figure 5b, the radar backscatter values from BS-50 and SH-51 are strongly correlated with snow depth between DOY 290 and DOY 341, Unfortunately we do not have radar data after DOY 341. Changes inradar backscatter from WS-52versus snow depth are less than in other tree species which is consistent with the fact that snow accumulation is less in closed canopies (WS) than in open canopies (BS and SH).

The radar backscatter curves corresponding to night and day pairs (that is, data available during an ascending/night pass for which a day/descending pass twelve hours later is also available) acquired during the 1991 Commissioning Phase are shown in Figure 3b. Diurnal changes in radar backscatter have been previously related to diurnal changes in the dielectric properties of Walnut trees (Way et al., 1991) using scatterometer measurements at L-, C-, and X- band frequencies, and may be linked to changes in water potential. Since we did not measure diurnal changes in the dielectric properties of the trees during the 1991 Commissioning Phase, we cannot correlate the ERS- 1 SAR observations shown in Figure 3b to changes in the dielectric properties of the trees. However, the fact that differences in radar backseat ter exist between day and night observations of the forest is encouraging that ERS-1 is sensitive to diurnal changes in the water content of the vegetation. ERS-1 SAR is designed to be very robust to changes in surface temperature of the antenna induced by changes in the amount of solar radiation that illuminates the satellite during day and night cycles (Attema, 1992a and 1992b; Woode et al., 1992), so that diurnal changes in radar backscatter observed in the summer over the forest stands of Manley are real, though less than 0.5 dB in magnitude. After DOY 260, the diurnal changes in radar backscatter are larger, up to 3 dB, and are attributed to partial freezing of the soil and vegetation at night due to sub-zero air-temperatures as discussed earlier. In contrast,

after DOY 300, diurnal changes in radar backscatter are the smallest, indicating almost no change in the dielectric properties of the soil and vegetation, which is consistent with the fact that the soil and vegetation are already frozen at that time of the year.

Figure 3b shows little separability between different types of forests when a number of different stands are considered. The variability in radar backscatter within stands of identical tree species is nearly as large as the separability in radar backscatter between stands corresponding to different tree species. In the summer WS and BP are not separable. BP has a higher radar backscatter than WS in the winter, but WS is then confused with sparse forests and shrub-lands. Combining multidate information does not significantly improve the separability between tree species. Several attempts at classifying the entire scene and at comparing the results with vegetation maps of the area did not yield good results. A complete assessment of ERS- 1 mapping capability requires however the examination of data acquired at different times of the year, in particular during Spring, As an example, Rignot and van Zyl (1992) showed that multi temporal ERS- 1 SA R data can separate forested areas from non-forested areas using a pair of images corresponding to frozen/winter conditions and thawed/spring conditions separated by 35-days.

8 CONCLUSIONS

For the first time, we have observed temporal changes in radar backscatter from boreal forests at C-band VV-polarization and at 3-day repeat interval in response to changing environmental conditions. The general observations agree well with radar backscatter model predictions. Due to the remarkable stability of ERS-1 SAR gain,

changes in radar backscatter at the 0.5 dB level are detected with confidence. Freezing of the soil and vegetation is easily detected as it yields drops in radar backscatter of about 3 dB, nearly independent of the type of vegetation cover. Periods of drying of the soil and vegetation after heavy rain falls yield 1 to 2 dB changes in radar backscatter which may also be detected, but for which interpretation is more difficult, Unexpectedly, radar backscatter values increase with increasing snow depth in winter, which may be due to the formation of large depth hoar ice crystals. In addition to these ERS-1 measurements, the SAR data acquired by AIRSAR in May 1991 over the Bonanza Creek Experimental Forest indicate that ERS-1 should also detect flooding of the forests during Spring break-up as radar backscatter values typically increase by 5 dB at C-band VV-polarization during periods of flooding compared to dry/frozen conditions (Way et al., 1992a).

These preliminary results indicate that there is potential for ERS- 1 SAR to monitor freeze-thaw transitions of the soil and vegetation of interior Alaska, relatively independent of the vegetation cover. Freeze/thaw events correspond to periods of dramatic changes in the heat balance between the surface and the vegetation (Weller and Holmgren, 1974), and also mark the end or beginning of photosynthetic activity for the vegetation. Monitoring freeze-thaw using ERS-1 SAR' data could therefore have important ecological implications. In a companion paper, Rignot and Way (1993) examined the possibility to extend those results to larger areas by detecting changes in radar backscatter over an entire North-South Alaskan transect of ERS- 1 SAR data, and the results are encouraging. More experience with temporal signatures of boreal forests acquired by ERS-1 will accumulate in years to come, and the ERS- 1 SAR observations will also be combined to the observations made by the Japanese first Earth Resources Satellite (J ERS-1), which operates at L-band frequency (λ = 24 cm),

HH-polarization, and 35° incidence angle, and for which the data are now becoming available.

Acknowledgements

This work was carried out at the Jet Propulsion Laboratory, California Instituteof Technology, under contract with the National Aeronautics and Space Administration. The authors would like to thank all the people from the Alaska SAR Facility, University of Fairbanks, Alaska, for receiving, processing, and distributing the ERS- 1 SAR data.

REFERENCES

Allen, C. T., Brisco, B., Ulaby, F.T. (1984), Modehngt hetemporal behavior of the microwave backscattering coefficient of agricultural crops, RSL Tech, Rep. 360-21, Remote Sensing Laboratory, Univ. of Kansas Center for Research, Inc., Lawrence, KS.

Attema, E. (1991), The active microwave instrument on-board the ERS- 1 satellite, *Proc. of the IEEE,* 79:791-799.

Attema, E. (1992a), *Personal* Communication, Nov. 1992.

Attema, E. (1992b), Science requirements for the calibration of the ERS- 1 Synthetic Aperture Radar, *Proc. CEOS SAR Calibration Workshop,* Ottawa, Canada, Sept. 21-25.

Dobson, M. C., McDonald, K. C., and Ulaby, F.T. (1989), Modeling of forest canopies and analysis of polarimetric SAR data, Radiation Laboratory Tech Report 026143-1-F, The University of Michigan Radiation Laboratory.

Dobson, M. C., McDonald, K., Ulaby, F. T., and Sharik, T. (1991), Relating the temporal change observed by AIRSAR to surface and canopy properties of mixed conifer and hardwood forests of northern Michigan, *Proc. of the 3rd airborne synthetic aperture radar (AIRSAR) workshop,* (van Zyl, J. J., Ed.), JPL Publication 91-30, Jet Propulsion Laboratory, Pasadena, CA, pp. 34-43,

Dobson, M. C., McDonald, K., Ulaby, F. T., Kasischke, E. S., and Way, J.B. (1993), Modeling the effects of temperature on microwave extinction and backscatter from a

boreal forest in winter, *IEEE Trans. on Geos. and Rem. Sens.*, In Press.

Carsey, F., and Weeks, W. (1987), The planned Alaska SAR Facility: an overview, *Proc. of the 1987 Int. Geosc. and Rem. Sens. Symp.,* IEEE Cat. 87 CH2434-9, Ann Arbor, MI, May 18-21, 1059-1062.

Elachi, C., Roth, L. E., and Schaber, G.G. (1984), Spaceborne radar subsurface imaging in hyperarid regions, *IEEE Trans. on Geosc. and Rem. Sens.*, 22:383-388.

Fatland, R., and Freeman, A. (1992), Calibration and change detection using Alaska SAR Facility ERS-1 SAR data, *Proc. of the 1992 Int. Geos. and Rem. Sens. Symp*, IEEE Cat. 92 CH3041-1, Houston, TX, May 26-29, 1164-1166.

Foote, M. J. (1983), Classification, description, and dynamics of plant communities after fire in the taiga of interior Alaska, Research Paper PNW-307, Portland OR, U. S. Department of Agriculture, Forest Service, Pacific Northwest Forest and Range Experiment Station, 108p.

Hall, D.K. (1988), Assessment of polar. climate change using satellite technology, *Rev. Geophysics,* 26:26-39.

Hallikainen, M., Ulaby, F. T., Dobson, M. C., El-Rayes, M., Wu, L.K. (1985), Microwave dielectric behavior of wet soil-part I: Empirical models and experimental observations, *IEEE Trans. on Geosc. and Rem. Sens.*, 23:25-34.

Juday, G. P., and Dyrness, C.T. (1985,), *Early results of the Rosie creek fire research project* (Juday and Dyrness, Eds.), Misc. Pub, 85-2, University of Alaska, Forest and Agriculture Experiment Station, Fairbanks, AK, 46p.

Kwok, R.., Rignot, E., Way, J. B., Freeman, A., and HoIt, J. (1993), Polarization signatures of frozen and thawed forests of varying environmental state, *IEEE Trans. on Geosc. and Rem, Sens.*, In Press.

Manabe, S., and Wetherald, R.T. (1980), On the distribution of climate change resulting from an increase in $C0_2$ content of the atmosphere, *J. of Atmos. Sci.*, 37:99-118.

Pruitt, W, O., Jr. (1984), Snow and living things, in *Northern Ecology and Resource Management* (R. Olsen et al., Eds.), The University of Alberta Press, pp. 51-77.

Rignot, E., and van Zyl, J. J., (1992), A comparison of change detection techniques using ERS-1 SAR data, *IEEE Trans. on Geosc. and Rem. Sens.*, Submitted.

Rignot, E., and Way, J.B. (1993), Monitoring freeze-thaw along North-South Alaskan transects using ERS-1 SAR, *Rem. Sens. Environ.*, Submitted.

Slaughter, C. W., and Viereck, L.A. (1986), Climatic characteristics of the taiga in interior Alaska, In Ecological Series *Vol. 57, Forest Ecosystems in the Alaskan Taiga* (van Cleve, K., Ed.), Springer-Verlag, NY, pp 2-21.

Sturm, M., and Johnson, J.B. (1992), Thermal conductivity measurements of depth hoar, *J. Geophys. Res.*, *97,* B2:2129-2139.

Trabant, D. C., and Benson, C.S. (1972), Field experiments on the development of depth hoar, In: *Studies of mineralogy and Precambrian geology,* (Doe, B. R., and Smith, D, K., Eds.), Geol. Sot. Amer., Memoir 135, pp. 309-322.

Ulaby, F. T., Moore, R, K., and Fung, A.K. (1982), Microwave *remote sensing: active and passive. Volume II: Radar remote sensing and surface scattering and* emission

theory, Addison-Wesley, Reading, MA.

Ulaby, F. T., El Rayes, M.A. (1987), Microwave dielectric spectrum of vegetation, Part II: dual-dispersion model, *IEEE Trans. on Geosc. and Rem. Sens.*, 25:550-557.

Ulaby, F. T., Sarabandi, K., McDonald, K., Whitt, M., and Dobson, D.C. (1990), Michigan Microwave Canopy Scattering Model, *Int. J. of Rem. Sens.*, 11:1223-1254.

Ulaby, F. T., Moore, R. K., and Fung, A.K. (1986), *Microwave remote sensing: active and passive. Volume III:* From *theory to applications,* Artech House, Dedham, MA,

van Cleve, K., and Viereck, L. A. (1981), Forest succession in relation to Nutrient cycling in the boreal forest of Alaska, In *Forest Succession: Concepts and Applications* (West, D. et al., Eds), Springer-Verlag Advanced Texts in Life Sciences, New York, pp. 185-211.

van Cleve, K., Oliver, L., Schlentner, R., Viereck, L. A., and Dyrness, C. T. (1983), Productivity and nutrient cycling in taiga forest ecosystems, *Can. J. For, Res.*, 13:747-766.

van Cleve, K., and Yarie, J. (1986), Interaction of temperature, moisture, and soil chemistry in controlling nutrient cycling and ecosystem development in the taiga of Alaska, In *Forest Ecosystems in the Alaskan Taiga* (K. van Cleve, et al,, Eds), Springer-Verlag, New York, pp. 160-189.

van Cleve, K., Chapin 111, F. S., Dyrness, C. T., and Viereck, L. A. (1991), Element cycling in taiga forests: state-factor control, *Bioscience, 41:78-88.*

van Zyl, J.J. (1989), Unsupervised classification of scattering behavior using radar

polarimetry data, *IEEE Trans. on Geosc. and Rem. Sens.*, 27:36-44.

van Zyl, J. J., Carande, R., Lou, Y., Miller, T., and Wheeler, K. (1992), The NASA/JPL three-frequency polarimetric AIRSAR system, *Proc. Intl. Geosc. and Rem. Sens. Symp.*, IEEE Cat. 92 CH3041-1, Houston, TX, May 26-29, 649-651.

Viereck, L. A., Dyrness, C. T., van Cleve, K., and Foote, M. J. (1983), Vegetation, soils, and forest productivity in selected forest types in interior Alaska, *Can. J. For. Res.*, 13:703-720.

Viereck, L. A., Dyrness, C. T., and van Cleve, K. (1986), Forest ecosystem distribution in the taiga environment, in *Forest Ecosystems in the Alaskan Taiga. A Synthesis of Structure and Function* (van Cleve, et al., Eds), Springer-Verlag, NY, pp 22-43,

Viereck, L, A., and Adams, P. (1990), Variation in microclimate among sites and changes of climate with time in Bonanza Creek Experimental Forest, *Proc. of the Long- Term Ecological Research Workshop into Climate Variability and Ecosystem Response,* Gen. Tech, Rep. SE-65 Asheville, NC, University of Colorado, Aug 21-23.

Waring, R. (1992), *Personal Communication,* Dec. *1992.*

Way, J. B., Paris, J., Kasischke, E., Slaughter, C., Viereck, L, A., Christensen, N., Dobson, M. C., Ulaby, F. T., Richards, J., Milne, A., Sieber, A. Ahern, F. J., Simonett, D., Hoffer, R., Imhoff, M., and Weber, J. (1990), The effect of changing environmental conditions on microwave signatures of forest ecosystems: preliminary results of the March 1988 Alaskan aircraft SAR experiment, *Int. J. Remote Sensing,* 11:1119-1144.

Way, J. B., Paris, J., Dobson, M. C., McDonald, K., Ulaby, F. T., Weber, J. A., Ustin, S. L., Vanderbilt, V. C., and Kasischke, E.S. (1991), Diurnal changes in trees as observed by optical and microwave sensors: The EOS synergism study, *IEEE Trans. on Geosc. and Rem. Sens., 29:807-821.*

Way, J, B., McDonald, K., Rignot, E., Bonan, G., Viereck, L., and Adams P. (1992a), Monitoring Temporal change in Alaskan forests using imaging radar: implications for estimating $C0_2$ flux, *Proc. of the 1992 Int. Geosc. and Rem. Sens. Symp*, IEEE Cat. 92 CH3041-1, Houston, TX, May 26-29, 1218-1219.

Way, J. B., Rignot, E., McDonald, K., Oren, R., Kwok, R., Bonan, G., Dobson, M. C., Viereck, L. A., and Roth, J. (1992b), Monitoring seasonal state and mapping species in Alaskan Taiga forests using imaging radars as in put to $C0_2$ flux models, *IEEE* Trans. *on Geosc.* and *Rem. Sens.*, In Press.

Way, J. B., McDonald, K., and Rignot, E. (1992 c), A novelist backscatter behavior of old balsam poplar stands in Bonanza Creek Experimental Forest, Alaska, In preparation.

Weller, G., and Holmgren, B. (1974), The microclimates of the Arctic tundra, *J. of Appl. Meteorol.*, 13:854-862.

Williams, C. (1992), Stand characteristics of Manley Hot Springs Ecosystem sites for ERS-1 Commissioning Phase ground truth data, Internal Report, Institute of Northern Forestry, Pub., Fairbanks, AK, 59 p.

Woode, A. D., Desnos, Y. L., and Jackson, H. (1992), The development of and first results from the ESTEC ERS- 1 active radar calibration unit, *IEEE Trans. on Geosc.*

and Rem. Sens., 30:1122-1130.

Zimmerman, R. (1993), In preparation.

LIST OF FIGURES

lines correspond to night passes and continuous lines correspond to day passes.

Figure 4: (a) Air-temperature (“C) in BS-50 versus DOY. The continuous curve corresponds to the air-temperatures at the times of ERS-1 day overpass, and the dotted curve corresponds to the air-temperatures at the times of ERS- 1 night overpass. Triangles and squares respectively indicate the dates of availability of ERS- 1 SAR data during a day and a night pass. Blanks correspond to missing data,; (b) Solar radiation ($\mu E/m^2$) in BS-50 versus DOY; (c) Soil temperatures (“C) in BS-50 at 10cm and 20cm depth versus DOY; (d) Precipitation rates (mm) recorded in the Manley forest sites on several dates;

Figure 5: (a) Precipitation rates (mm) recorded at Tanana versus DOY; (c) Snow depth (cm) recorded at Tanana versus DOY. Triangles indicate the dates of availability of ERS-1 SAR data during a day pass.

Figure 6: Real part of the dielectric constant of trees at 4 different depths (bark (0. 0cm), phloem (0.3cm), cambium(0.6cm), xylem (1.6cm)) versus DOY for (a) BS-50; (b) BP-51; and (c) WS-52.

Figure 7: Gravimetric moisture content of the leaves, wood, inner-bole, and outer-bole for (a) BS-50; (b) BP-51; and (c) WS-52. Gravimetric moisture content of the understory, litter, moss, organic soil, and mineral soil for (d) BS-50; (e) BP-51; and (f) WS-52.

Figure 8: ERS-1 radar backscatter values predicted by MIMICS versus the real part of the dielectric constant of the woody material ϵ_r for different values of the volumetric soil moisture (%) with (a) BS-50; (b) BP-51; (c) WS-52. The different values of soil moisture are indicated on the right of the corresponding radar backscatter curve.

Contributions to the total radar backscatter (solid lines) of 3 dominant scattering mechanisms (direct scattering from the crown is shown in dotted lines; direct scattering from the ground is shown in dashed lines; and scattering from trunk-ground interactions is shown in dash-dotted lines) for very wet soil (soil moisture = 40 %) and very dry soil (soil moisture = O %) with (d) BS-50; (e) BP-51; (f) WS-52.

Figure 9: ERS- 1 radar backscatter predicted from a radiative transfer model where the snow comprises thin fresh snow grains at the top and depth hoar ice crystals at the bottom, over a ground surface with a rms height of 0.5 cm and a correlation length of 2 cm, Fresh snow grains are 0.5mm in size. ERS- 1 radar backscatter is plotted for different depth hoar ice crystal sizes versus the height of the depth hoar layer, keeping the total snow depth constant equal to 20cm.

LIST OF TABLES

SITE	STEMS	Cover	Basal Area	Mean DBH	Mean HT	BIOMASS
	# / h a	%	m^2/ha	cm	m	kg/ha
BS-50	1370	23	4.9	6.5	5.1	11401
BP-51	1060	71	42.5	22,5	20.1	174033
WS-52	654	41	24.8	21.3	16.7	113644

Table 1: Tree data summarized bystands, means often plots.

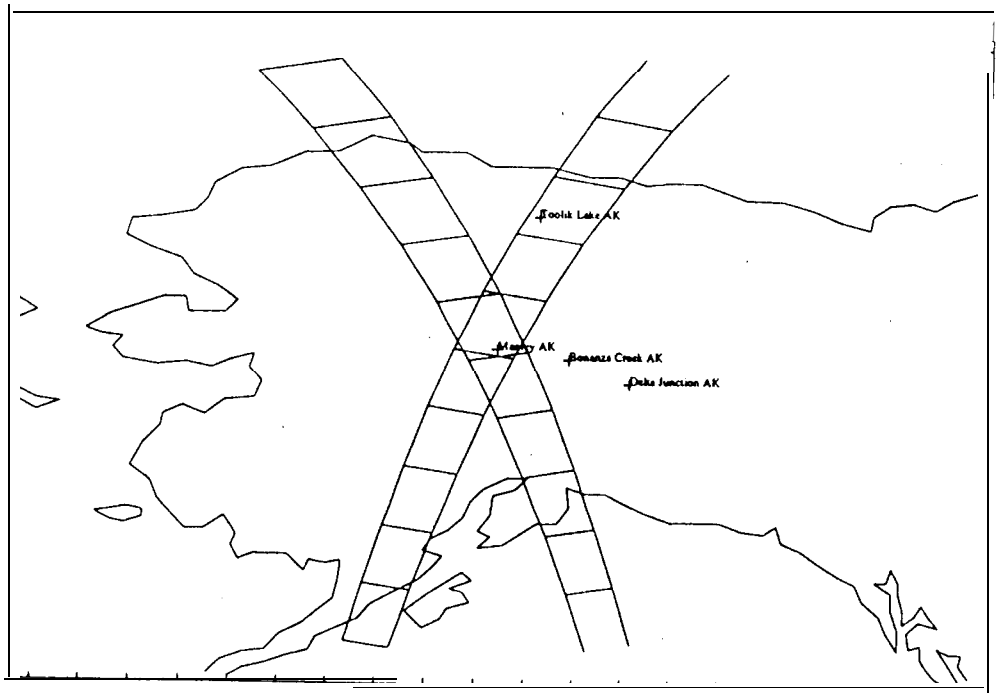

Figure 1.

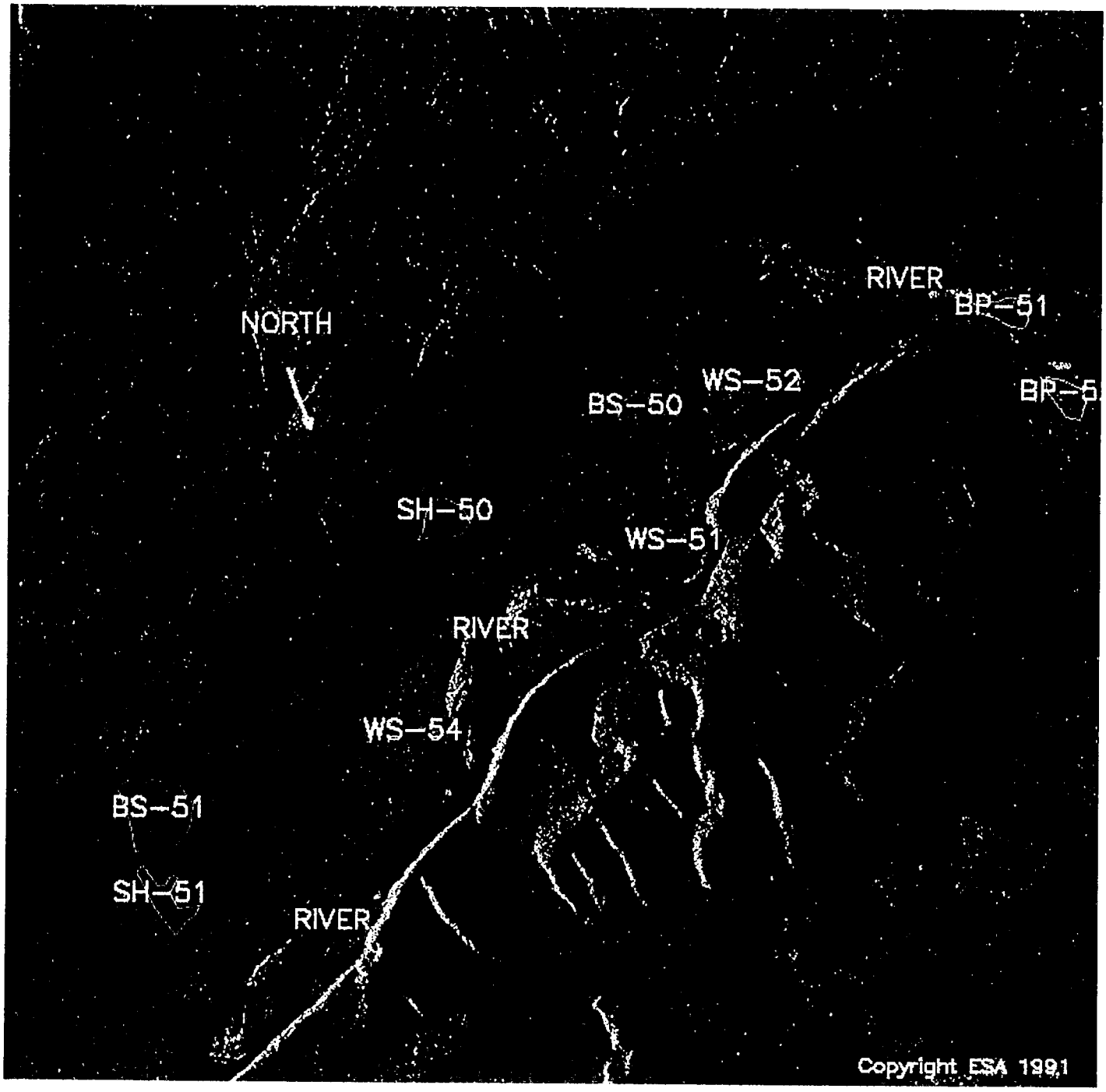
RIVER
BP-51
NORTH
WS-52
BS-50
SH-50
WS-51
RIVER
WS-54
BS-51
SH-51
RIVER
Copyright ESA 1991

Figure 2.

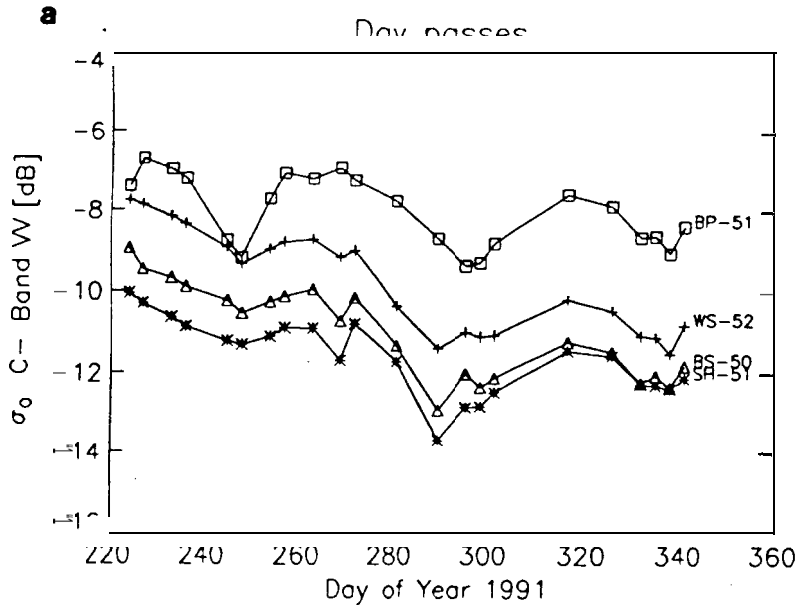
a
Day passes
σo C- Band VV [dB]
-4
-6
-8
-10
-12
-14
BP-51
WS-52
BS-50
SA-51
220
240
260
280
300
320
340
360
Day of Year 1991

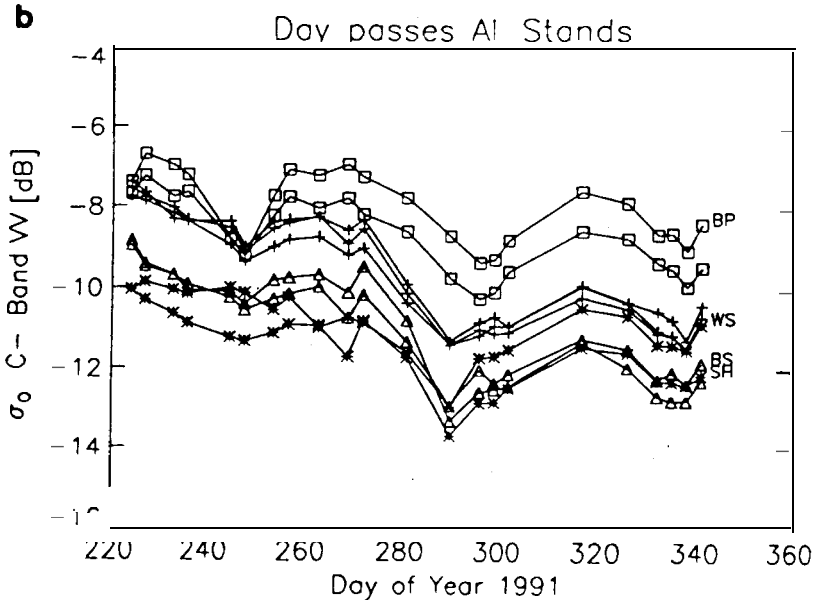
b
Day passes Al Stands
σo C- Band VV [dB]
-4
-6
-8
-10
-12
-14
BP
WS
BS
SA
220
240
260
280
300
320
340
360
Day of Year 1991

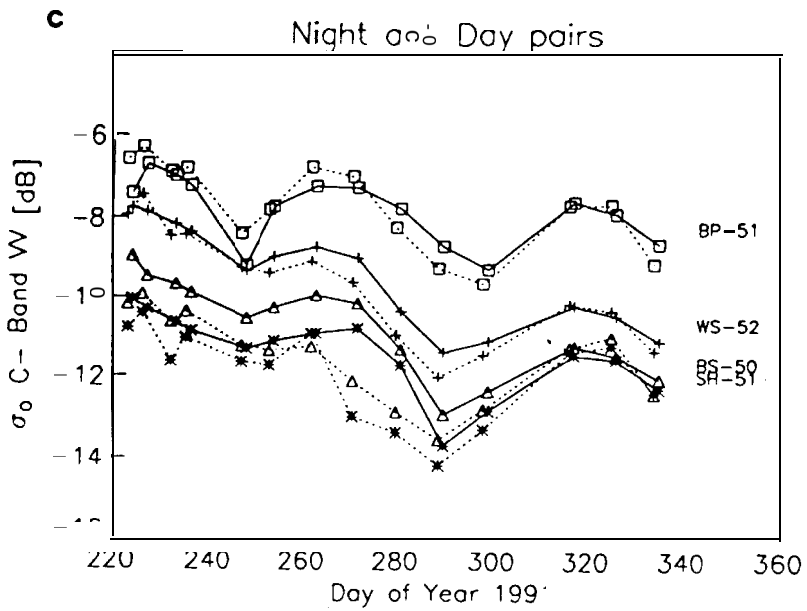
c
Night and Day pairs
σo C- Band VV [dB]
-6
-8
-10
-12
-14
BP-51
WS-52
BS-50
SA-51
220
240
260
280
300
320
340
360
Day of Year 199

Figure 3.

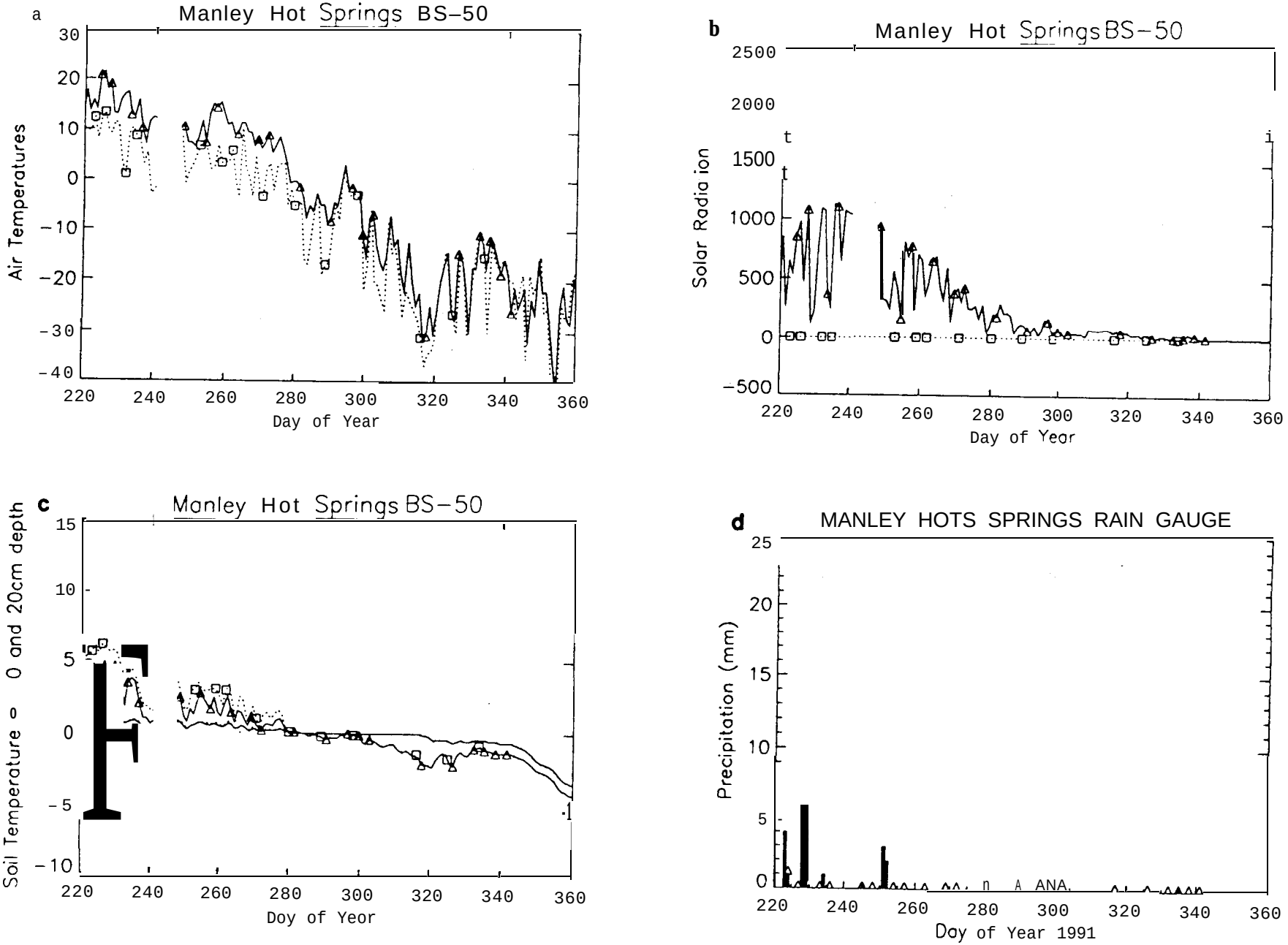
a
Manley Hot Springs BS-50
Air Temperatures
Day of Year
b
Manley Hot Springs BS-50
Solar Radia ion
Day of Yeor
c
Manley Hot Springs BS-50
Soil Temperature o 0 and 20cm depth
Doy of Yeor
d
MANLEY HOTS SPRINGS RAIN GAUGE
Precipitation (mm)
Day of Year 1991

Figure **4.**

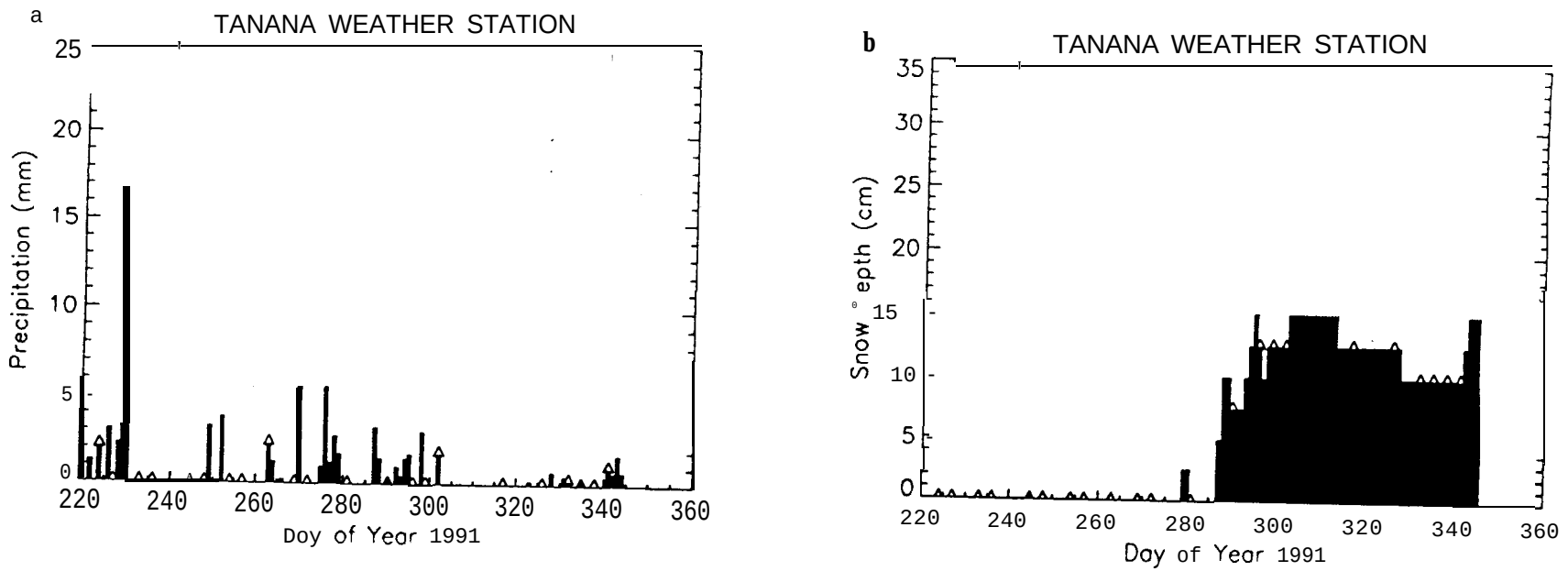
a
TANANA WEATHER STATION
Precipitation (mm)
25
20
15
10
5
0
220
240
260
280
300
320
340
360
Doy of Year 1991
b
TANANA WEATHER STATION
Snow Depth (cm)
35
30
25
20
15
10
5
0
220
240
260
280
300
320
340
360
Day of Year 1991

Figure 5.

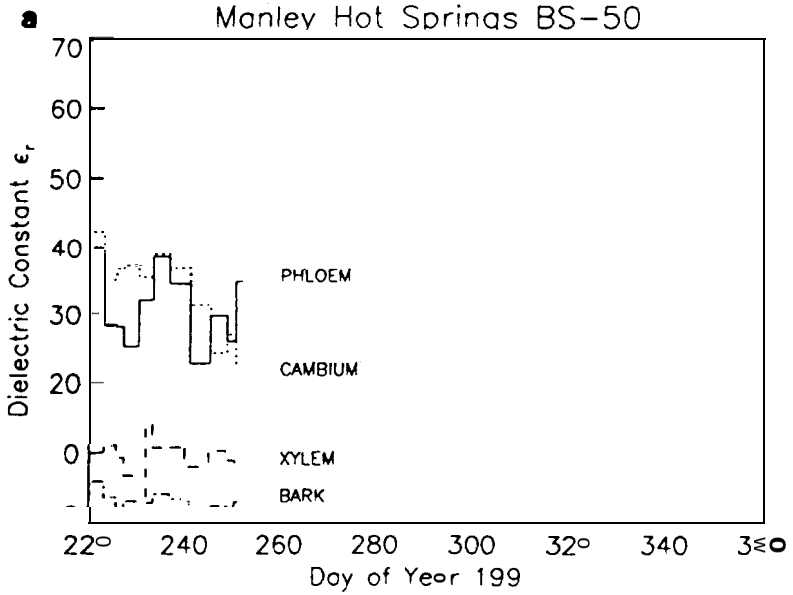
a
Manley Hot Springs BS-50
Dielectric Constant ϵ_r
70
60
50
40
30
20
0
PHLOEM
CAMBIUM
XYLEM
BARK
22°
240
260
280
300
32°
340
Day of Year 199

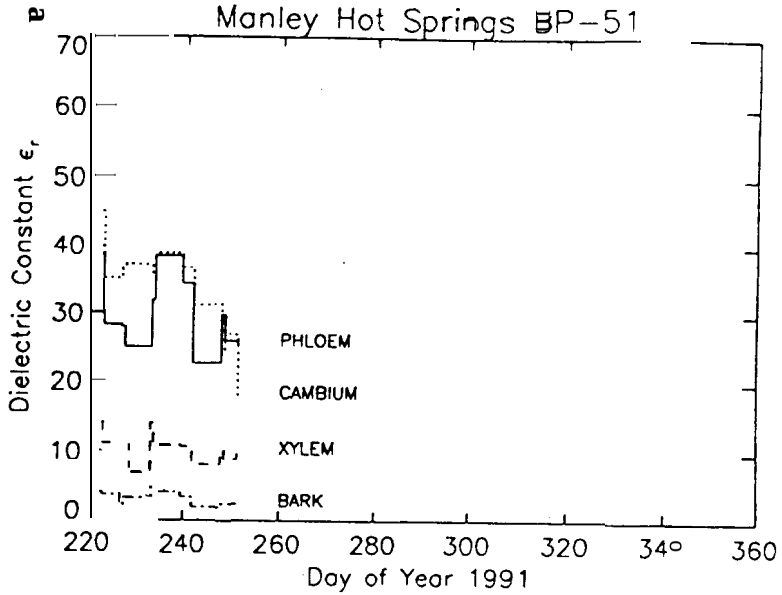
b
Manley Hot Springs BP-51
Dielectric Constant ϵ_r
70
60
50
40
30
20
10
0
PHLOEM
CAMBIUM
XYLEM
BARK
220
240
260
280
300
320
34°
360
Day of Year 1991

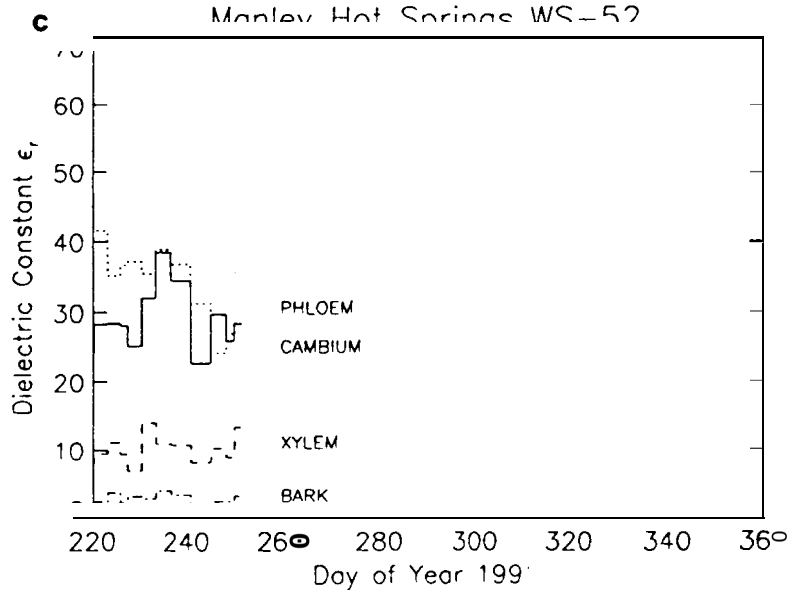
c
Manley Hot Springs WS-52
Dielectric Constant ϵ_r
60
50
40
30
20
10
PHLOEM
CAMBIUM
XYLEM
BARK
220
240
260
280
300
320
340
36°
Day of Year 199

Figure 6.

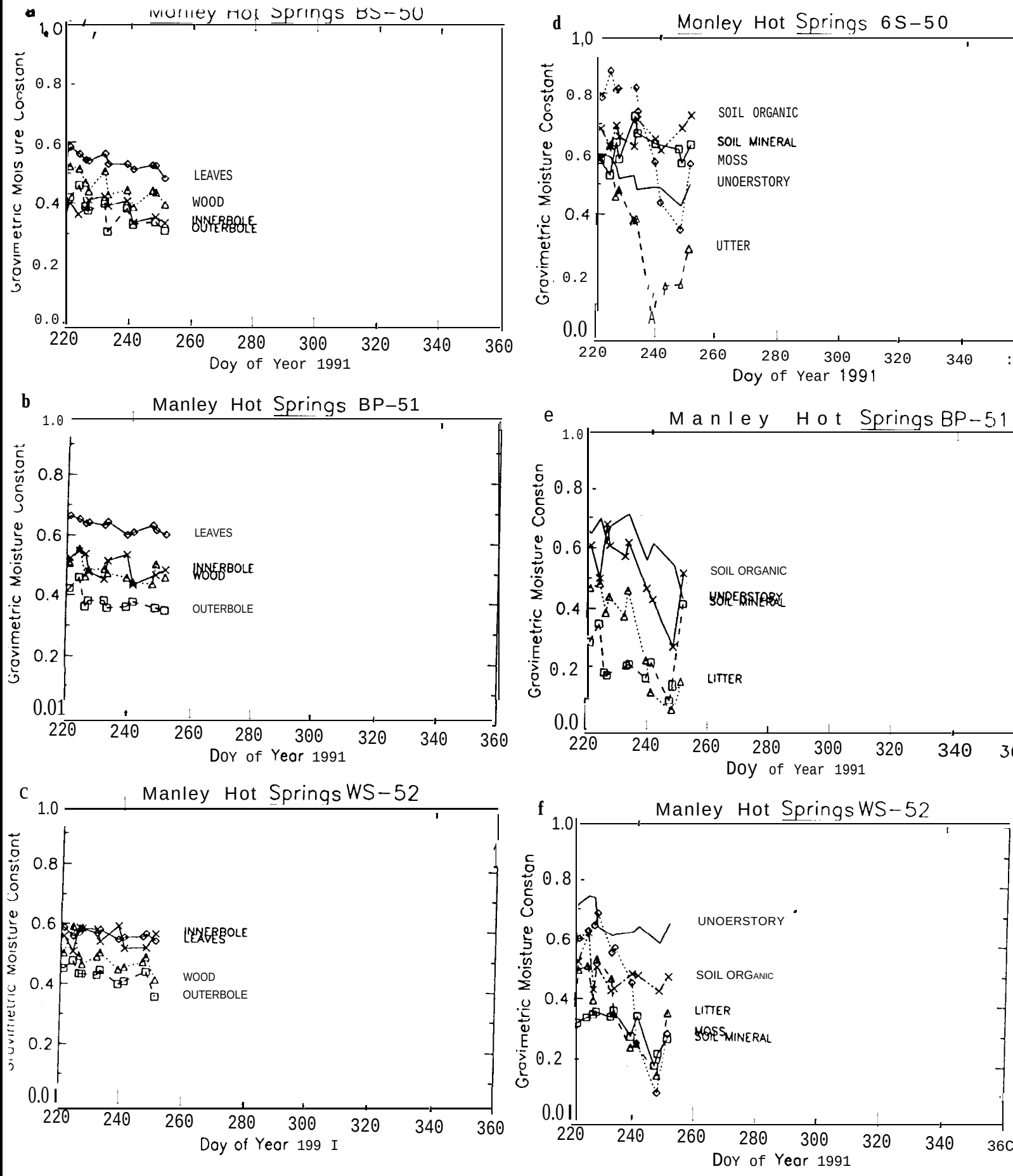
a
Manley Hot Springs BS-50
Gravimetric Moisture Constant
LEAVES
WOOD
INNERBOLE
OUTERBOLE
Day of Yeor 1991
b
Manley Hot Springs BP-51
Gravimetric Moisture Constant
LEAVES
INNERBOLE
WOOD
OUTERBOLE
DOY of Year 1991
c
Manley Hot Springs WS-52
Gravimetric Moisture Constant
INNERBOLE
LEAVES
WOOD
OUTERBOLE
Day of Year 199 I
d
Manley Hot Springs 6S-50
Gravimetric Moisture Constant
SOIL ORGANIC
SOIL MINERAL
MOSS
UNOERSTORY
UTTER
Day of Year 1991
e
Manley Hot Springs BP-51
Gravimetric Moisture Constan
SOIL ORGANIC
UNOERSTORY
SOIL MINERAL
LITTER
Doy of Year 1991
f
Manley Hot Springs WS-52
Gravimetric Moisture Constan
UNOERSTORY
SOIL ORGANIC
LITTER
MOSS
SOIL MINERAL
DOY of Year 1991

Figure 7.

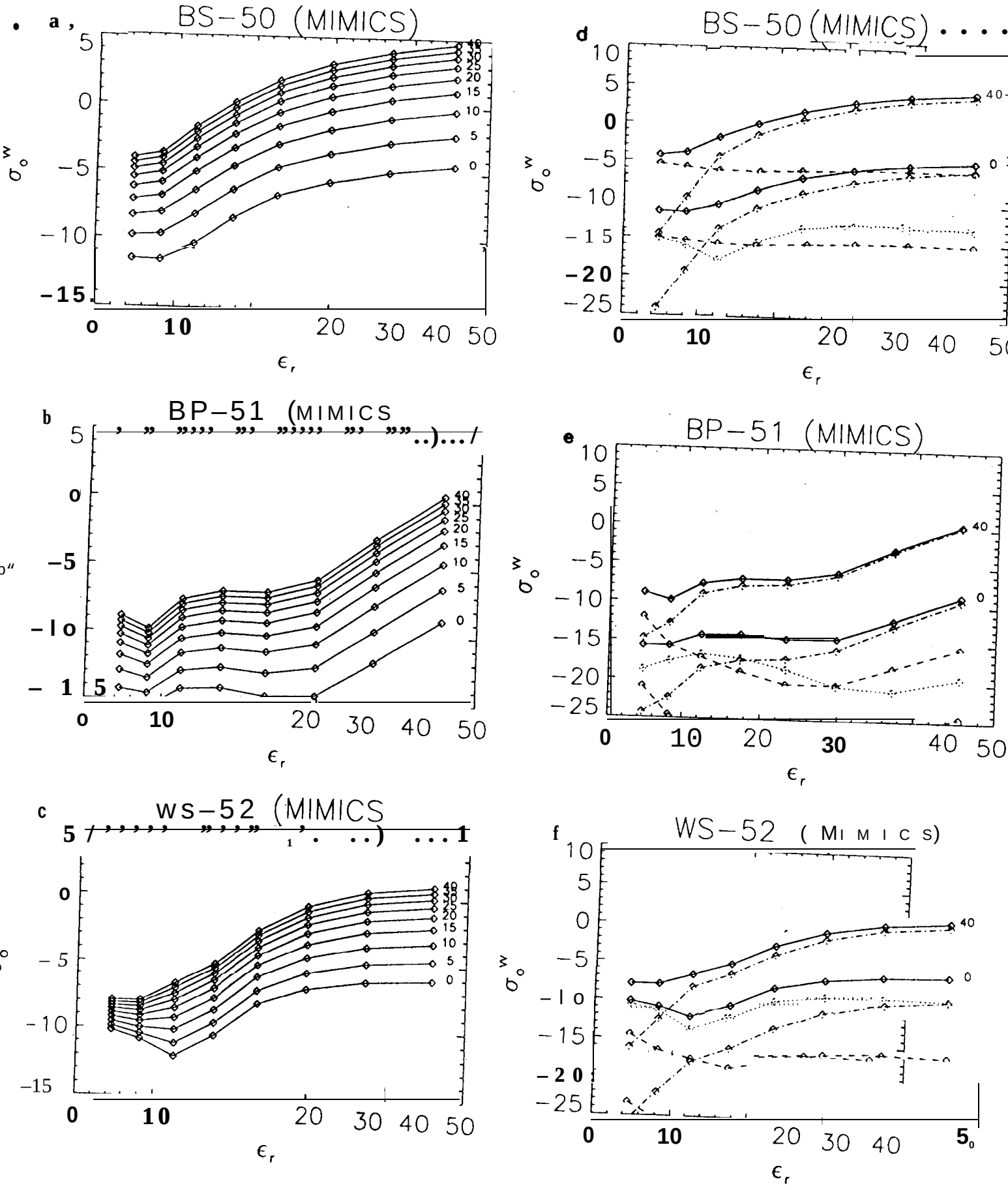
a
BS–50 (MIMICS)
d
BS–50 (MIMICS)
b
BP–51 (MIMICS
e
BP–51 (MIMICS)
c
ws–52 (MIMICS
f
WS–52 (MI M I C S)
σ_o^w
ϵ_r
40
30
25
20
15
10
5
0

Figure 8.

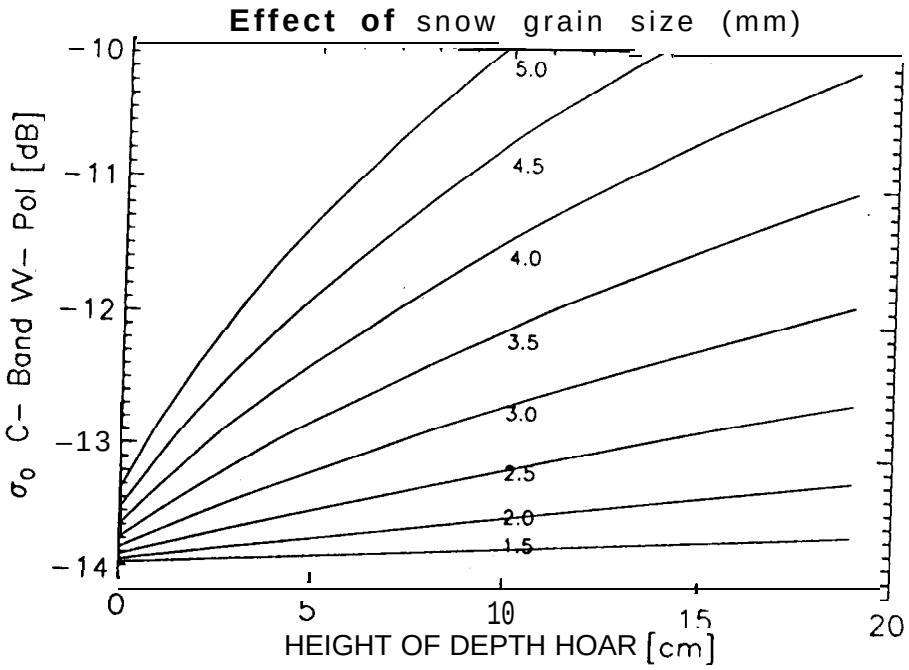
Effect of snow grain size (mm)
−10
−11
−12
−13
−14
σo C− Band W− Pol [dB]
5.0
4.5
4.0
3.5
3.0
2.5
2.0
1.5
0
5
10
15
20
HEIGHT OF DEPTH HOAR [cm]

Figure 9.